China Instrument and Control Society
Instrumentation
OPEN ACCESS
INSTRUMENTATION, Vol. 13, No. 3, September 2026 https://doi.org/10.15878/j.instr.202600380

Articles

Research on A Simple Analysis Method for Aqueous Solution Via Total Reflection X-Ray Fluorescence and Argon Peak Normalization

Kuan Wang[1], Xiao Fu[1*], Fajie Duan[1], Jiajia Jiang[1], Jingxin Wu[2]

[1] State Key Lab of Precision Measuring Technology & Instruments, Tianjin University, Tianjin, 300072, China

[2] Design of Aeroengine Compressor Structure, AVIC Hunan Power Machinery Research Institute, Zhuzhou, Hunan, 412002, China

[*] Corresponding author email: fuxiao215@tju.edu.cn, ORCID: 0000-0002-2221-2878

Abstract: The commonly used internal standard method process for total reflection x-ray fluorescence (TXRF) is too cumbersome for online analysis. The accuracy of the method using argon peak in air as normalization standard is tested. It is compared with external standard method and Compton scattering line normalization method. The calibration curve was established using Ga standard solution. For the results of the argon peak normalization and external standard method, the correlation coefficients were 0.9995. For the results of the argon peak normalization and Ga peak normalization, the correlation coefficients were 0.997. The argon peak and Compton peak at different incident angles were compared. At the total reflection angle, the stability of the argon peak in low concentration samples is better than that of the Compton scattering line peak. This provides a theoretical basis for a simple analysis method of aqueous solutions based on argon peak normalization.

Keywords: TXRF; sample preparation; aqueous solution; Ar normalization; external standard methods

Copyright: © 2026 by the authors. This article is licensed under a Creative Commons Attribution 4.0 International License (CC BY) license (https://creativecommons.org/licenses/by/4.0/).

Citation: Kuan Wang, Xiao Fu, Fajie Duan, Jiajia Jiang, Jingxin Wu. "Research on A Simple Analysis Method for Aqueous Solution Via Total Reflection X-Ray Fluorescence and Argon Peak Normalization." Instrumentation 13, no.3 (September 2026). https://doi.org/10.15878/j.instr.202600380

1 Introduction

X-ray fluorescence (XRF) is a rapid and non-destructive element detection method, which is widely used in the fields of environmental detection, ore detection and biological detection[1-3]. It has irreplaceable advantages in the field of industrial large-scale online element detection[4-6]. However, the detection limit of an XRF spectrometer limits its application in the field of trace element detection[7]. On the basis of XRF, total reflection x-ray fluorescence (TXRF) element detection method was developed[8]. TXRF has the advantages of high precision, low detection limit and simple sample preparation, and can be used for trace element detection[9-11]. However, the TXRF element analysis method requires a certain sample preparation process and cannot be applied to large-scale online element detection[12]. In practical applications, there is a need for on-line detection of trace elements in environmental sewage monitoring, ore screening monitoring and oil monitoring[13-15]. As a result, exploring efficient online TXRF methods is imperative. Amauri A. Menegario and colleagues coupled a flow system with reduced pre-concentration to TXRF multi-element determination[16]. The addition of internal standards and online pre-concentration reduced both handling and analysis time. Junior Ma and the team proposed a quantitative online analytical scheme using TXRF for simultaneous trace heavy metal analysis in the environment[17]. However, the arduous process involved in preparing samples is a primary obstacle that impedes online analysis through TXRF.

The common methods for quantitative detection of trace elements in TXRF include internal standard method, external standard method and scattering line normalization method[18-20]. The commonly used internal standard method process for TXRF is too cumbersome

for online analysis. Jinfa Shao et al.'s proposed normalization method, which utilizes argon peaks, yielded quantitative analysis outcomes for plant samples that are comparable to those achieved through the internal standard method, but without the need to introduce internal standard elements[21]. If the online TXRF analysis method, which employs Ar normalization, boasts high accuracy, then the process of sample preparation - involving weighing, the addition of internal standard, shaking, and dropping - can be simplified[22,23]. This simplification facilitates the implementation of TXRF online analysis. However, this simplification process is also suitable for the external standard method and the scatter normalization method. For external standards, the determination of quantitative concentration intervals and the acquisition of the reference material are challenging. For scattering line internal standard, a suitable scattering ray must be selected, usually using Compton scattering. It is not clear whether the argon peak normalization method is more competitive.

In this work, the argon peak signal as an internal standard quantitative method was compared with the external standard method, Compton scattering normalization and internal standard method. The signal intensity of different sample deposition was obtained by the method of sample on-site enrichment. The analysis results of argon peak normalization were compared with those of external standard method and Compton scattering normalization. Gallium was used as the internal standard element to compare the results of argon peak normalization and internal standard analysis. The research provides a theoretical basis for simplifying the preparation process of TXRF samples and realizing on-line analysis of TXRF.

2 Materials and Methods

2.1 Materials and Experiments

2.1.1 Instruments

The main devices of the apparatus include a side window X-ray tube (Mo target, 50 kV, 1 mA), a waveguide slit (10 mm × 30 mm × 0.06 mm), and a silicon drift detector (SDD, 30 mm^2, 8 μm Be window, FWHM = 128 ± 3 eV @ 5.9 keV). The X-ray tube was mounted on the precision displacement stage through clamps and on the precision tilt stage using right-angle fixing blocks. The height and inclination of the X-ray tube are adjusted by means of a precision displacement stage and a precision tilt stage. The waveguide structure is mounted on the precision tilt stage to correct for small angles due to processing errors, and the slit is constructed by two silicon wafers with a roughness of less than 0.5 nm and an aluminum foil in the middle. A silicon wafer with a surface roughness of less than 0.5 nm was used as the sample reflector for the test, and the X-ray incidence angle was adjusted using the precision tilt stage, with the silicon drift detector probe aligned with the center of the precision tilt stage. During the tests, the protective ring of the probe was very close to the sample, and the Be window was less than 3 mm from the sample. To operate for an extended period, the X-ray tube did not function at full power. The best detection limit of 149 pg (in 10 μL of a 1 mg/L single-element Ga standard solution) was obtained for 1000 s of Ga testing at a tube voltage of 35 kV and a tube current of 800 μA. All tests were performed in an air atmosphere.

2.1.2 Samples, Reagents and Standards

The standard solutions used in the experiment include Ga standard solutions (1 ppm in 3% HNO_3 and 100 ppm in 5% HNO_3) and Ca standard solutions (100 ppm in 5% HNO_3). The reagents used in the experiment include ultrapure water used to dilute the standard solutions. Ga standard solutions and aqueous solutions were used to test the stability of the method. The 100 ppm Ga standard solutions and Ca standard solutions were diluted with ultrapure water to test the accuracy of the method. By depositing the sample repeatedly over a small area of the sample reflector, different portions of the sample were deposited in similar areas to obtain the concentration of the element to be measured in the same volume of solution deposited at different multiples of the sample used. These samples were used to establish the relationship between the signal of the element to be measured in the sample and the argon peak area, thus obtaining the sensitivity of the element to be measured relative to Ar for the same matrix.

2.1.3 Sample Preparation and Analysis

In order to compare the conditions applicable to the argon peak and the normalization of the elemental scattering rays on the target surface of the X-ray tube, all tests were performed at an X-ray tube voltage of 35 kV and a tube current of 800 μA. Since the sample reflector is a silicon wafer with hydrophobicity, no siliconization was performed using a silanol solution. The samples were pipetted with 10 μL drops onto the silicon wafer and dried in a thermostat at 70 ℃ for 5 min to obtain deposits with a small area. The samples were deposited using the same pipette, and only 10 μL of liquid was added. In order to analyze the deposits at a position close to the bottom of the SDD probe, the flat groove of the silicon wafer was used to fix the position of the silicon wafer, and the sample was added dropwise near the fixed point. Due to the drift in the sensitivity of the SDD probe to photons, the longer the analysis time, the more stable it becomes. To maximize the signal intensity of the weak signal, a test time of 600 s was adopted with consideration for experimental efficiency.

2.2 Theory and Methodology

2.2.1 Theoretical

Jinfa Shao et al. have demonstrated that the Ar

normalization method is feasible in TXRF, and according to the theory of the Ar normalization method, samples of unknown concentration are detected by the method of[21]

$$C_i = \frac{N_i}{N_{Ar}} \frac{C_{Ar}}{R_{i,Ar}} \quad (1)$$

where C_i is the concentration of element i in the sample, $R_{i,Ar}$ is the relative sensitivity of the analyte to the argon peak, and N_i and N_{Ar} are the peak area counts of element i and Ar in the sample, respectively. The peak area counts of Ar have nothing to do with the analyte, but only with the relative sensitivity of the analyte to the argon peaks under the same analytical conditions. Under ideal conditions, the relationship between N_i and C_i under the same analytical conditions is as follows

$$N_i = KC_iV_i \quad (2)$$

where K is the scale factor under ideal conditions and V_i is the volume of analyte deposited on the sample reflector. When performing TXRF experiments, the higher the concentration and volume of the sample, the larger the area of deposited evaporites. In the ideal case, the concentration and volume of the sample deposited have a negligible effect on the counting results. Since C_{Ar} remains stable in air and $R_{i,Ar}$ is stable under the same test conditions, the following relationship exists at this time

$$K_{Ar}kC_i = \frac{N_{kvi}}{N_{Ar}} = \frac{N_{kci}}{N_{Ar}} \quad (3)$$

where K_{Ar} is a constant, N_{kvi} is the peak area count deposited at k times the volume compared to the original sample, and N_{kci} is the peak area count deposited at k times the concentration compared to the original sample. A linear relationship can be obtained by the least squares method through the ratio of element i peak area counts to argon peak area counts for a set of standard samples. Also, a similar relationship can be obtained for element i peak area counts for different deposition amounts of a given sample. Therefore, as long as the ratio of element i peak area count to argon peak area count at a certain concentration of a sample is obtained, the ratio of element i peak area count to argon peak area count of a group of standard samples can be obtained, and under the same analytical conditions, samples of other concentrations can be quantitatively analyzed. The relationship between quantitative curves is shown in Fig. 1. The volume of a single drop is 4-20 μL. The linear range of the standard curve can be adjusted using the automatic pipetting device. The standard curve can be generated by analyzing standard samples.

2.2.2 Comparison of Analytical Methods

The main source of the SDD detector signal in the TXRF is shown in Fig. 2. The scattering of the original X-ray on the material around the SDD probe is the background source, and the Compton scattering is generated. In the air atmosphere, the Ar gas around the bottom of the SDD probe produces an Ar characteristic peak. In the dry matter with a small area under the SDD probe, the element i to be measured and the internal

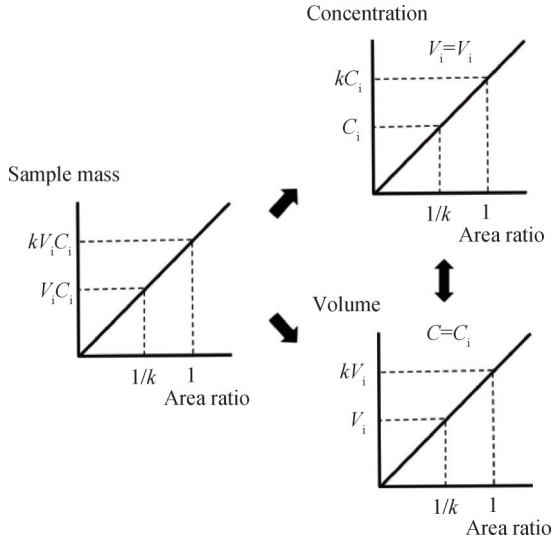


Fig.1 The relationship between quantitative curves

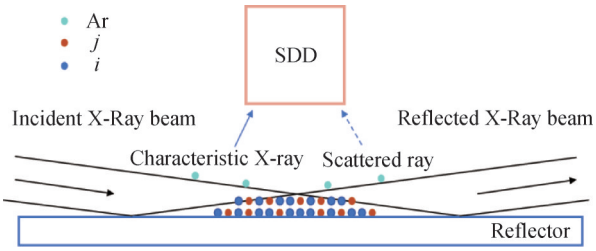


Fig.2 Schematic diagram of the source of the detection signal

standard element j produce i characteristic peak and j characteristic peak. Due to the slight difference in the area of the sample dry matter and the position relative to the detector during actual operation, the accuracy of the quantitative analysis of the internal standard method is the highest.

The samples analyzed by TXRF usually require infinite thinness, in which case the matrix effect can be ignored. When the thickness of the sample exceeds the critical value, the matrix effect generated is mainly absorption effect, resulting in attenuation of the signal of the tested element in the sample. Due to the similar matrix effect between the tested element i and the internal standard element j, the internal standard method can to some extent suppress the matrix effect. The increase in sample thickness will lead to a decrease in Ar above the sample. Due to the narrow standing wave of X-rays generated by the overlap of incident and reflected X-rays, a significant increase in sample thickness can lead to a decrease in Ar signal. Therefore, within a certain thickness range of the sample, the ratio of the measured signal to the Ar signal can effectively correct the matrix effect, achieving a similar effect as the internal standard method, that is

$$\frac{A_i}{A_j} \approx \frac{A_i}{A_{Ar}} \approx 1 \quad (4)$$

where A_i is the attenuation rate of i, A_j is the attenuation rate of j, A_{Ar} is the attenuation rate of Ar. Previous work has shown that the linearity of TXRF

detection results is closely related to the morphology of sample deposition[24]. Compared to water-based samples where the sediment is mainly composed of metal cations, oil-based samples may contain a large amount of low-Z elements in the sediment. Oil-based samples with the same concentration usually have thicker sediment on the sample stage than water-based samples. Thinner samples usually have better linear results[25]. Due to the better detection limit obtained by evaporation enrichment of low boiling point oil-based samples, the enrichment method used in this method is also applicable to low boiling point oil-based samples[26]. However, it is more likely that formula (4) will fail due to the inconsistency between the decay of the tested element and Ar caused by excessively high sample concentration. For low concentration and water-based samples, enrichment within 5 times can achieve better detection limits. For higher concentration and oil-based samples, less sample usage should be used to obtain thinner sample deposition morphology and avoid samples exceeding the applicable range of this method. At this point, there will be nonlinearity between the sample deposition amount and the detection results. This in turn can also identify whether the test sample is suitable for this method.

The position of the SDD detector is usually fixed, and the external standard method also has good accuracy when the inclination and position of the reflector are unchanged. Compton scattering normalization is used to correct the analysis results of low Z samples by external standard method in TXRF. Compared with the external standard method, the Compton scattering peak normalization method can effectively correct instrument drift and matrix effects. This is because Ar is also affected by the enhanced absorption effect. The Compton scattering peaks of elements on the target surface of an X-ray tube are typically utilized. However, low-power X-ray sources typically cannot generate reliable Compton scattering peak. The argon peak normalization method quantifies the ratio of the argon peak to the peak area of the element being measured. Compared with the internal standard method, this method cannot correct the error caused by the small change of the sample dry matter. Compared with the external standard method, this method corrects the error caused by the performance fluctuation of X-ray tube and SDD detector, and brings the error of argon peak fluctuation. Compared with Compton scattering normalization, this method has a stable argon peak and is not limited by the conditions of Compton scattering peak generation. The experiment will further compare these methods.

3 Results and Discussion

Due to the rapid increase in the Si peak signal with the increase in grazing angle, and the relative stability of the argon peak signal after reaching the critical angle of total reflection at the grazing angle[21]. During the process of increasing the grazing angle from near the critical angle of total reflection, the ratio of the Si peak signal to the argon peak signal continuously increases. This ratio can be used to indicate the increase in grazing angle. Low-concentration gallium standard samples are used as test samples. The signal from the X-ray tube is utilized as the scattering peak. The grazing angle gradually increases as it approaches the critical angle of total reflection. During this process, the changes in signal intensity of Si, Ar, Ga, and Mo are shown in Fig. 3.

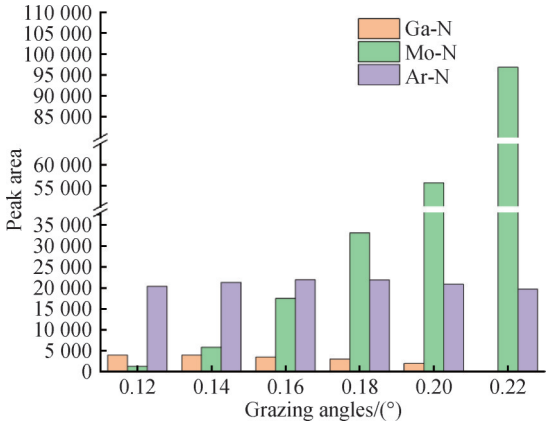


Fig.3 Changes in signal intensity of Ar, Ga, and Mo during the increase in grazing angle (Ar-N, Ga-N, Mo-N are the signal area counts of Ar, Ga and Mo peaks, respectively)

During the process of increasing the grazing angle, the argon peak signal is very stable. The signal of the Si peak rapidly increases, leading to a significant rise in the ratio of the Si peak signal to the argon peak signal. This ratio is used as the abscissa in the graph to illustrate the process of increasing the grazing angle. The scattered Mo peak signal starts small and then gradually increases. The peak signal of the element being tested starts to stabilize relatively and then decreases rapidly. The specific data is shown in Table 1.

Table 1 Signal area counts of Si, Ar, Ga, and Mo peaks at different grazing angles

Grazing angles (°)	N_{Si}/N_{Ar}	N_{Si}	N_{Ar}	N_{Ga}	N_{Mo}
0.12	0.6478	13191	20362	3929	1186
0.14	2.443	52025	21297	3923	5780
0.16	5.515	120964	21933	3446	17503
0.18	9.797	214485	21892	2935	33166
0.20	24.93	520357	20871	1912	55673
0.22	38.64	762001	19719	n.d.	96801

Note: N_{Si}, N_{Ar} , N_{Ga} , N_{Mo} are the signal area counts of Si, Ar, Ga and Mo peaks, respectively. N_{Si}/N_{Ar} is the ratio of Si peak signal to argon peak signal. The n. d. indicates that it exceeds the detection limit.

According to the results shown in Fig. 3, the relationship between the signal and the grazing angle can

be obtained. As the grazing angle increases, it transitions from a total reflection state. The signal strength of the tested element Ga gradually decreases. It is worth noting that the scattered Mo peak is relatively weak near the critical angle of total reflection. Due to instrument drift, the stability of weak signals is compromised. This will seriously affect the stability of the detection results. The low sample concentration, small grazing angle, and low X-ray tube power collectively result in weak scattered signals. In this case, the argon peak normalization method is more suitable than the scattering line normalization method.

When the diffusion of droplets changes, it will affect the thickness of sample deposition. It is obvious that this not only affects the signal of the tested element and the magnitude of the matrix effect, but also affects the volume of air within the standing wave range, thereby affecting the Ar signal. Fortunately, for low concentration samples, the deposition of the samples is similar under the same sample preparation method. The impact caused by different sedimentation conditions can be ignored[24]. The samples with varying amounts of deposited Ga were analyzed, and the results are shown in Fig. 4. As depicted in the figure, there is no Ga signal in the sample without Ga deposition. The Ga signal counting area increases with the increase in the number of samples deposited. The signal counting area of other elements in the samples, such as Ca (3.69 keV), increases, while the argon peak signal remains more stable. The relative standard deviation (RSD) of the argon peak signal in five sets of data is 1.2%, but it will decrease to less than 1% when conducting a large number of experiments. The detailed data are shown in Table 2. The least-squares regression of the Ga deposition fraction with NGa/NAr, NGa, and NGa/NMo was performed, and the results are shown in Fig.5.

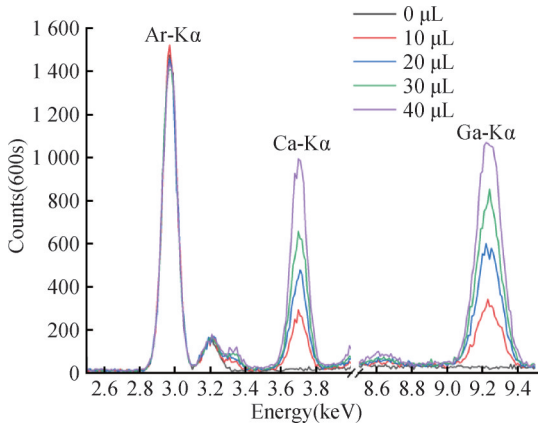


Fig.4 Spectra results for various Ga deposition amounts

From the data in Fig.4, Fig.5 and Table 2, it can be seen that N_{Ar} is relatively stable, and the variation of N_{Ga}/N_{Ar} is very close to that of N_{Ga}. The correlation coefficient between the argon peak normalization method and the external standard method analysis results is 0.9995. The regression coefficients of N_{Ga}/N_{Ar} and Ga

Table 2 Signal area counts of Ar, Ga, and Mo peaks with different Ga deposits

Deposition volume (μL)	N_{Ga}	N_{Ga}/N_{Ar}	N_{Ga}/N_{Mo}
0	0	0	0
10	4284±169	0.297±0.015	5.02 ±0.24
20	8025±240	0.575±0.020	8.98 ±0.32
30	11180±367	0.797±0.030	10.97 ±0.47
40	15350±338	1.086±0.027	13.14 ±0.49

Note: N_{Si} , N_{Ar} , N_{Ga} , N_{Mo} are the signal area counts of Si, Ar, Ga and Mo peaks, respectively. The values are means of four measurements ± standard deviation.

deposition fraction, R^2, are 0.9978, and those of N_{Ga} and Ga deposition fraction, R^2, are 0.9975. These values are very close to each other, indicating a strong linearity. This indicates that the multiple depositions of samples at similar positions did not significantly affect the analysis of the samples. The small change in the center point of the sample deposition position and the increase in the area of the dry matter fall within a certain range. Additionally, the number of photons obtained by the detector during the analysis remains similar. At the same time, the on-site enrichment method did not significantly affect the Ga signal counting area by increasing the sample thickness within a certain range. The specified conditions meet the requirements for applying the argon peak normalization method when the ratio of NGa/NAr demonstrates a strong linear correlation with the Ga content in the sample. In this concentration range, using a set of standard samples of the same volume can result in a better linear fit. Therefore, the argon peak normalization method can achieve similar accuracy to the external standard method within the range of the maximum deposition volume of a set of standard samples for which the correction factor was determined by least squares.

The effect of multiple deposition of samples on the stability of the test results was tested. The concentrations of Ca and Ga in the samples are constant. The sample was deposited four times, each time depositing 10 μL sample. The internal standard method was used to quantify the concentration of Ca by the ratio of the peak area of Ca and Ga. The argon peak normalization method quantifies the concentration of Ca by the ratio of the peak area of Ca to Ar and the volume of sample deposition. The external standard method was used to quantify the concentration of Ca according to the peak area of Ca and the volume of sample deposition. The correlation between the normalization of Ca concentration argon peak and the analysis results of internal standard method under different volumes of the same sample is shown in Fig. 6. For Ca in solution, the repeatability results of internal standard method, argon peak normalization, and external standard method for the same sample analysis under different sample deposition volumes are shown in

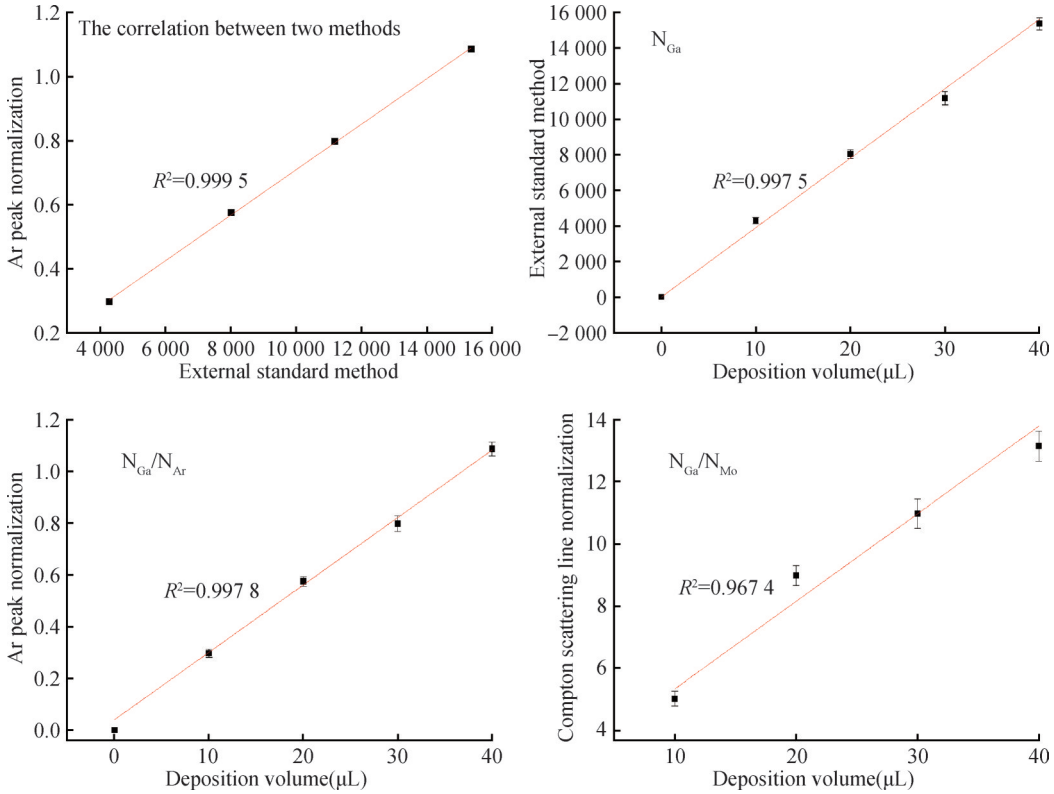


Fig.5 Effect of linear fitting of N_{Ga}/N_{Ar}, N_{Ga} and N_{Ga}/N_{Mo} with Ga deposition fraction (Ar peak normalization is N_{Ga}/N_{Ar} of sample from 10 μL to 40 μL; External standard method is N_{Ga} of sample from 10 μL to 40 μL; N_{Ar} , N_{Ga} , N_{Mo} are the signal area counts of Ar, Ga and Mo peaks, respectively. The values are means of four measurements ± standard deviation.)

Table 3 Repeatability of internal standard method, argon peak normalization, and external standard method

Analysis methods	Deposition volume (μL)	Corresponding value	Convert the value of 10 μL	Limit of detection (μg L^{-1})	Average value	Standard deviation	RSD (%)	Recovery (%)
Internal standard method	10	0.609	0.609	0.018	0.620	0.038	6.2	105
	20	0.585	0.585	0.011				
	30	0.610	0.610	0.007				
	40	0.674	0.674	0.006				
argon peak normalization	10	0.181	0.181	0.018	0.174	0.010	5.8	97
	20	0.336	0.168	0.011				
	30	0.487	0.162	0.007				
	40	0.732	0.183	0.006				
External standard method	10	2610	2610	0.018	2455	169	6.9	97
	20	4698	2349	0.011				
	30	6822	2274	0.007				
	40	10352	2588	0.006				

Table 3. The formula for the calculation of TXRF LOD is given in Eq. (5) [26] where c_i is the concentration of element i, I_{BG} is the intensity of the background region below the fluorescence peak, and I_{peak} is the intensity of the fluorescence peak region.

$$LOD = \frac{3 \cdot c_i \cdot \sqrt{I_{BG}}}{I_{peak}} \quad (5)$$

Due to the negligible impact of adding low concentration internal standards on the results, according to the detection limit formula, the detection limits of the three methods are the same. With the increase of enrichment times, the decrease in detection limit is no longer significant. The detection limits of 30 μ L and 40 μ L samples are very close. The maximum enrichment times for water-based samples generally do not exceed 5 times, while the maximum effective enrichment volume for

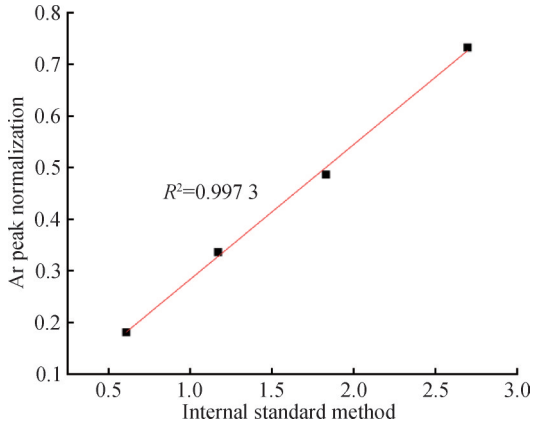


Fig.6 The correlation between argon peak normalization and Internal standard method analysis results (argon peak normalization is N_{Ca}/N_{Ar} of the sample volume from 10 μL to 40 μL; Internal standard method is $N \times N_{Ca}/N_{Ga}$ of the sample volume from 10 μL to 40 μL; N_{Ar} , N_{Ga} , N_{Ca} are the signal area counts of Ar, Ga and Ca peaks, respectively; N is the number of sample depositions)

oil-based samples is smaller[26]. From the data in Fig. 6 and Table 3, the normalized results of argon peak are very close to those of gallium peak. The correlation coefficients between the results for the argon peak normalization and the results for Ga peak normalization were 0.997. The regression coefficient R^2 between N_{Ga}/N_{Mo} and Ga sediment fraction is 0.94. The zero point seriously deviates from the standard curve. After removing the zero point, the R^2 is 0.96. Compared to the argon peak normalization method, the Compton scattering line normalization method has poorer stability. Due to the low signal intensity of Compton scattering, the signal detected by the detector is not stable. However, the stability of the average of multiple results has greatly improved. Due to the instability of Compton scattering signals, the argon peak normalization method is more stable than the Compton scattering normalization method. On the other hand, when using high-concentration samples for experiments, the N_{Mo} significantly increases, and detection errors decrease significantly. In addition, if the grazing angle is slightly increased, N_{Mo} can be significantly increased. If the power of the X-ray tube is high enough, better scattering peaks can also be obtained.

Based on the above study, the argon peak normalization method is suitable for analyzing low-concentration elements in solutions using TXRF. The Ga signal intensity, after Ar normalization, shows a strong linear correlation with the Ga content. However, the argon peak normalization method requires a known injection volume and the same operating conditions as the standard. Deviations in the injection volume and the position of the dryer can introduce systematic errors, leading to poorer analytical accuracy compared to the internal standard method. The internal standard method is more suitable for TXRF analysis under various conditions. However, the cumbersome sample preparation required by the internal standard method hinders its promotion for online analytical applications. The external standard method and the scattering ray normalization method are more suitable for scenarios where a simplified sample preparation process is required. However, in the external standard method, determining quantitative concentration linear intervals and accessing the same standards can be challenging. When using internal standards with scattered peaks, it can be challenging to identify the appropriate scattered rays when employing low-power multicolor X-rays. Therefore, the argon peak, which is stable in air, is more suitable for replacing the scattered peak and normalizing the quantitative analysis of the element to be measured. This method simplifies the sample processing process and has reference value for the application of TXRF technology in detection where internal standards cannot be added to avoid contamination and in fields that require rapid detection.

4 Conclusion

The study confirms the feasibility of the argon peak normalization method by verifying the linear relationship between the Ar-normalized Ga signal intensity and the deposited Ga content within the confirmed boundary conditions. Although the quantitative analysis accuracy is not as good as that of the internal standard method, this method is an effective sample preparation process, overcomes the difficulties in determining the quantitative concentration intervals of the traditional external standard method and the acquisition of the same standard material, and reduces the error due to the difference in sensitivity between the standard samples and the samples to be tested for the elements to be measured. The stable argon peak is utilized in the case of difficulty in obtaining suitable scattering rays, and the quantitative analysis is carried out by Ar normalization drawing on the scattering ray normalization method. The feasibility of simplifying the TXRF sample preparation method based on the argon peak normalization method was discussed through comparative experiments. The experimental results indicate that within a certain concentration range, this method can be used to directly detect aqueous solutions without the need for additional sample preparation processes. This will help TXRF technology to be better applied in the detection of chips that cannot add internal standards and in the field of water quality and environmental detection that requires rapid detection.

Author Contributions:

Kuan Wang: Conceptualization; Validation; Writing-original draft; Writing-review & editing. Xiao Fu: Methodology; Supervision; Funding acquisition; Writing-review & editing. Fajie Duan: Supervision; Funding acquisition; Project administration. Jiajia Jiang: Supervision; Funding acquisition. Jingxin Wu: Validation; Software.

Funding Information:

This work was supported in part by National Natural Science Foundation of China under Grant (U2241265, 92360306, U25A20292, 52575633, 52575634), High-end Instruments and Equipment Program (20251.6XT213-001), AECC Outsourced Project (GJCZ-0202-2024-0006、GJCZ-0202-2024-0004、 GJCZ-0202-2024-0010), Tianjin National Key Laboratory Major Project (24ZXZSSS0 0290).

Data Availability:

The authors declare that the main data supporting the findings of this study are available within the paper and its Supplementary Information files.

Conflicts of Interest:

The authors declare no competing interests.

Ethics Statement

Not applicable.

Use of Generative AI and AI-Assisted Technologies

No generative AI was used.

References

[1] McIntosh K. G., Cordes N. L., Patterson B. M., & Havrilla G. J. (**2015**). Laboratory-based characterization of plutonium in soil particles using micro-XRF and 3D confocal XRF. *Journal of Analytical Atomic Spectrometry,* 30(7), 1511-1517. doi:10.1039/c5ja00068h

[2] Zuber A., Purdey M., Schartner E., Forbes C., Van der Hoek B., Giles D., Abell A., Monro T. & Ebendorff-Heidepriem, H. (**2016**). *Detection of gold nanoparticles with different sizes using absorption and fluorescence based method. Sensors and Actuators B*: Chemical, 227, 117-127. doi: 10.1016/j.snb.2015.12.044

[3] Wu S., Dong L., Ji J., Zhao P., Song G., Wu X., Jifeng W., Yunfeng Z., & Wang J. (**2023**). Simultaneous detection of trace As, Hg, Tl, and Pb in biological tissues using monochromatic excitation X-ray fluorescence spectrometry. *Journal of Analytical Atomic Spectrometry,* 38(10), 2127-2133. doi:10.1039/d3ja00127j

[4] Ringo M. C., Huhta M. S., Shea-McCarthy G., Penner-Hahn J. E., & Evans C. E. (**1999**). *On-line X-ray fluorescence detection for capillary electrophoresis separations*. Nuclear Instruments and Methods in Physics Research Section B: Beam Interactions with Materials and Atoms, 149(1-2), 177-181. doi:10.1016/S0168-583X(98)00889-1

[5] Yan Z., XinLei Z., WenBao J., Qing S., YongSheng L., DaQian H., & Da C. (**2016**). Online X-ray fluorescence (XRF) analysis of heavy metals in pulverized coal on a conveyor belt. *Applied spectroscopy,* 70(2), 272-278. doi: 10.1177/0003702815620129

[6] Ben Amar I., Thomas A., Bachmann C., Hafnaoui A., Griguer H., Miled A., & Messaddeq Y. (**2023**). XRF online analyzer for measurements of P2O5 content in phosphate slurry. *Scientific reports,* 13(1), 17925. doi:10.1038/s41598-023-45181-5

[7] McComb J. Q., Rogers C., Han F. X., & Tchounwou P. B. (**2014**). Rapid screening of heavy metals and trace elements in environmental samples using portable X-ray fluorescence spectrometer, a comparative study. *Water, Air, & Soil Pollution,* 225, 1-10. doi:10.1007/s11270-014-2169-5

[8] Wobrauschek P. (**1998**). Total reflection X-ray fluorescence spectrometric determination of trace elements in the femtogram region: a survey. *Journal of Analytical Atomic Spectrometry,* 13(5), 333-337. doi:10.1039/a707116g

[9] Liu Y., Imashuku S., & Kawai J. (**2013**). Multi-element analysis by portable total reflection X-ray fluorescence spectrometer. *Analytical Sciences,* 29(8), 793-797. doi: 10.2116/analsci.29.793

[10] Bilo F., Cirelli P., & Borgese L. (**2023**). Elemental analysis of particulate matter by X-ray fluorescence methods: A green approach to air quality monitoring. *TrAC Trends in Analytical Chemistry,* 117427. doi:10.1016/j.trac.2023.117427

[11] Kunimura S., Hatakeyama S., Sasaki N., Yamamoto T., & Kawai J. (**2010**). *Portable TXRF Spectrometer with* 10^{-11} g Detection Limit and Portable XRF Spectromicroscope with Sub‐mm Spatial Resolution. In AIP Conference Proceedings (Vol. 1221, No. 1, pp. 24-29). American Institute of Physics. doi:10.1063/1.3399251

[12] Ardid M., Ferrero J. L., Juanes D., Lluch J. L., & Roldán C. (2004). Comparison of total-reflection X-ray fluorescence, static and portable energy dispersive X-ray fluorescence spectrometers for art and archeometry studies. Spectrochimica Acta Part B: Atomic Spectroscopy, 59(10-11), 1581-1586. doi:10.1016/j.sab.2004.03.013

[13] Li Y., Chang M., Ding S., Wang S., Ni D., & Hu H. (**2017**). Monitoring and source apportionment of trace elements in $PM_{2.5}$: Implications for local air quality management. *Journal of environmental management,* 196, 16-25. doi: 10.1016/j.jenvman.2017.02.059

[14] Patel A. K., Chatterjee S., & Gorai A. K. (**2019**). Development of a machine vision system using the support vector machine regression (SVR) algorithm for the online prediction of iron ore grades. *Earth Science Informatics,* 12, 197-210. doi:10.1007/s12145-018-0370-6

[15] Yuwei Y., Wei J., Dan Z., Tao Z., Yangwei Y., Jin S., Xuchen Z., Bingwen Y., Ting C., Zhao L. & *Qinhan, J.* (**2018**). Application of Kilowatt MPT-AES in Oil Analysis. Chemical Journal of Chinese Universities, 39(12), 2651-2657. doi: 10.7503/cjcu20180377

[16] Menegario A. (**2003**). *On-line preconcentration flow system for multi-elemental analysis by total reflection X-ray fluorescence spectrometry* . Spectrochimica Acta Part B: Atomic Spectroscopy, 58(3), 543-549. doi: 10.1016/s0584-8547(03)00010-7

[17] Ma J., Wang Y., Yang Q., Liu Y., & Shi P. (**2015**). Intelligent Simultaneous Quantitative Online Analysis of Environmental

Trace Heavy Metals with Total-Reflection X-Ray Fluorescence. *Sensors,* 15(5), 10650-10675. doi:10.3390/s150510650

[18] Dhara S., Khooha A., Singh A. K., Tiwari M. K., & Misra N. L. (**2018**). *Total reflection X-ray Fluorescence determination of interfering elements rubidium and uranium by profile fitting.* Spectrochimica Acta Part B: Atomic Spectroscopy, 144, 87-91. doi:10.1016/j.sab.2018.03.011

[19] Pashkova G. V., Aisueva T. S., Finkelshtein A. L., Cherkashina T. Y., & Shchetnikov A. A. (**2018**). Quantitative approaches to the determination of elements in lake sediments by total reflection X-ray fluorescence. *Microchemical Journal,* 143, 264-271. doi:10.1016/j.microc.2018.08.020

[20] Sanyal K., Dhara S., Gumber N., & Pai R. V. (**2023**). A highly sensitive method for uranium quantification in water samples at ultra-trace level by total reflection X-ray fluorescence, after its direct pre-concentration on the surface of amidoxime functionalized quartz sample supports. *Talanta,* 254. doi: 10.1016/j.talanta.2022.124129

[21] Shao J., Jia W., Zhang X., Liu Y., Tang X., Xiong G., & Shan Q. (**2020**). Analysis of plant samples by low-power total reflection X-ray fluorescence spectrometry applying argon-peak normalization. *Journal of Analytical Atomic Spectrometry,* 35(4), 746-753. doi:10.1039/c9ja00419j

[22] De La Calle I., Cabaleiro N., Romero V., Lavilla I., & Bendicho C. (**2013**). Sample pretreatment strategies for total reflection X-ray fluorescence analysis: A tutorial review. *Spectrochimica Acta Part B-Atomic Spectroscopy,* 90, 23-54. doi:10.1016/j.sab.2013.10.001

[23] Sanyal K., & Dhara S. (**2023**). *Recent advances in ultra-trace determination of uranium in natural water using total reflection X-ray fluorescence (TXRF) spectrometry.* X-Ray Spectrometry. doi:10.1002/xrs.3379

[24] David Hellin, Wim Fyen, Jens Rip, Tinne Delande, Paul W. Mertens, Stefan De Gendt, Chris Vinckier. (**2004**). Saturation effects in TXRF on micro-droplet residue samples. J. Anal. At. *Spectrom,* 19 (12): 1517-1523. doi:10.1039/b410643a.

[25] Mercedes Regadío, Sofía Riaño, Koen Binnemans, Tom Vander Hoogerstraete. (**2017**). Direct Analysis of Metal Ions in Solutions with High Salt Concentrations by Total Reflection X-ray Fluorescence. Anal. *Chem,* 89 (8): 4595-4603. doi:10.1021/acs.analchem.7b00097.

[26] Cinosi A., Andriollo N., Pepponi G., Monticelli D. (**2011**). A novel total reflection X-ray fluorescence procedure for the direct determination of trace elements in petrochemical products. *Anal Bioanal Chem,* 399, 927-933. doi: 10.1007/s00216-010-4352-x.